HHS Public Access

Author manuscript

Nanomedicine. Author manuscript; available in PMC 2023 May 19.

Published in final edited form as:

Nanomedicine. 2020 October ; 29: 102257. doi:10.1016/j.nano.2020.102257.

A nanovaccine formulation of *Chlamydia* recombinant MOMP encapsulated in PLGA 85:15 nanoparticles augments CD4+ effector (CD44high CD62Llow) and memory (CD44high CD62Lhigh) T-cells in immunized mice

Rajnish Sahu, MSc, PhD[a], **Saurabh Dixit, PhD**[a,1], **Richa Verma, PhD**[a], **Skyla A. Duncan, PhD**[a], **Mamie T. Coats, PhD**[a,2], **Guillermo H. Giambartolomei, PhD**[b], **Shree R. Singh, PhD**[a], **Vida A. Dennis, PhD**[a,*]

[a]Center for NanoBiotechnology & Life Sciences Research, Department of Biological Sciences, Alabama State University, Montgomery, AL, USA

[b]Instituto de Inmunología, Genética y Metabolismo (INIGEM), CONICET, Universidad de Buenos Aires, Buenos Aires, Argentina

Abstract

Vaccine developmental strategies are utilizing antigens encapsulated in biodegradable polymeric nanoparticles. Here, we developed a *Chlamydia* nanovaccine (PLGA-rMOMP) by encapsulating its recombinant major outer membrane protein (rMOMP) in the extended-releasing and self-adjuvanting PLGA [poly (D, L-lactide-co-glycolide) (85:15)] nanoparticles. PLGA-rMOMP was small (nanometer size), round and smooth, thermally stable, and exhibited a sustained release of rMOMP. Stimulation of mouse primary dendritic cells (DCs) with PLGA-rMOMP augmented endosome processing, induced Th1 cytokines (IL-6 and IL-12p40), and expression of MHC-II and co-stimulatory (CD40, CD80, and CD86) molecules. BALB/c mice immunized with PLGA-rMOMP produced enhanced $CD4^+$ T-cells-derived memory ($CD44^{high}$ $CD62L^{high}$), and effector ($CD44^{high}$ $CD62L^{low}$) phenotypes and functional antigen-specific serum IgG antibodies. *In vivo* biodistribution of PLGA-rMOMP revealed its localization within lymph nodes, suggesting migration from the injection site *via* DCs. Our data provide evidence that the PLGA (85:15) nanovaccine activates DCs and augments *Chlamydia*-specific rMOMP adaptive immune responses that are worthy of efficacy testing.

Keywords

PLGA [poly (D, L-lactide-co-glycolide)] nanoparticles; Biodistribution; Dendritic cells trafficking; T-cells and antibody responses; *Chlamydia*

*Corresponding author. vdennis@alasu.edu (V.A. Dennis).

[1]National Institute of Allergy and Infectious Disease, Integrated Research Facility, Department of Clinical Research, 8200 Research Plaza, Ford Detrick, MD, 21702, USA.

[2]Current address: Clinical and Diagnostic Science Department, The University of Alabama at Birmingham, Birmingham, AL, 35294, USA.

Appendix A. Supplementary data

Supplementary data to this article can be found online at https://doi.org/10.1016/j.nano.2020.102257.

In recent years, subunit vaccines based on minimal elements of the pathogen are increasingly becoming a dogma.[1] Studies have shown that the use of biodegradable polymeric nanoparticles as delivery vehicles for subunit vaccines enhances the immunogenicity of the antigens by improving their uptake.[2,3] PLGA [poly (D, L-lactide-co-glycolide)] has been studied extensively as a nanomedicine delivery vehicle.[4–6] because of its extended-release of antigens to selectively target dendritic cells (DCs) and improve intracellular delivery *via* CD40 costimulation to activate T-cells.[7–9]

Chlamydia trachomatis is the most reported bacterial sexually transmitted infection globally, with over 100 million infections per year.[10,11] Development of a *Chlamydia* vaccine is critical to reducing the prevalence of infection, the socio-economic burden associated with diagnosis and treatment, and providing relief in the *Chlamydia*-induced sequelae such as infertility, pelvic inflammatory disease, and ectopic pregnancy.[12–14] Our vaccine efforts are focused on biodegradable self-adjuvanting polymeric nanoparticles as delivery vehicles for *Chlamydia* subunit vaccines, especially its major outer membrane protein (MOMP).[15] MOMP is an immunogenic abundantly expressed surface-exposed protein that triggers T-cell responses and neutralizing antibodies.[16]

Our previous nanovaccine design using *Chlamydia* recombinant MOMP (rMOMP) encapsulated in PLGA (50:50; lactide: glycolide ratio) nanoparticles had a low encapsulation efficiency (EE); yet it induced *in vitro* and *in vivo* Th1 immune responses.[17] Contrastingly, a *Chlamydia* peptide encapsulated in the extended-releasing PLGA (85:15) nanoparticles had a high EE that also stimulated Th1 immune responses *in vitro*.[18] Here, we designed a new *Chlamydia* nanovaccine by encapsulating rMOMP into PLGA (85:15) for its extended-releasing and high EE attributes. We hypothesized that PLGA (85:15) delivery of the immunogenic MOMP would augment Th1 immune responses correlating with *Chlamydia* protective immunity. To address our hypothesis, we first characterized the PLGA-rMOMP nanovaccine using a variety of nanotechnology techniques. Next, we employed primary mouse bone marrow-derived DCs as antigen-presenting cells (APCs) to evaluate the extended-release as well as activation and intracellular processing of the nanovaccine to trigger key cytokines, chemokines, co-stimulatory, and surface molecules. Next, we performed *in vivo* live imaging to reveal the biodistribution of the nanovaccine in mice. Finally, we immunized mice to assess the capacity of our nanovaccine to trigger cellular and antibody adaptive immune responses. We present and discuss our results in the context of PLGA (85:15) being an efficient delivery system and robust immunepotentiator of our *Chlamydia* nanovaccine.

Methods

The details of the materials and methods are in the supplementary file.

Preparation of nanoparticles

C. trachomatis rMOMP was cloned and encapsulated in PLGA (85:15) biodegradable nanoparticles (PLGA-rMOMP) using a water/oil/water double emulsion evaporation technique.[19]

Encapsulation efficiency (EE) and protein loading capacity (LC)

The EE was extrapolated from the quantification of the total rMOMP encapsulated in PLGA nanoparticles.[17] The LC was calculated based on the amount of rMOMP in PLGA-rMOMP.[18] Calculations of the EE and LC were conducted using the formulas below, where A is the total amount of rMOMP, B is the free rMOMP amount, and C is the weight of nanoparticles.

$$EE\ (\%) = \left[\frac{A-B}{A}\right]100$$

$$LC\ (\%) = \left[\frac{A-B}{C}\right]100$$

Physical-structural characterization studies

The zeta-sizing and zeta-potential of nanoparticles were measured using Nano-ZS (Malvern Instruments Ltd., Malvern, UK) and reported as the mean size in diameter (nm) and zeta-potential (mV).[17,18] Ultraviolet spectroscopy (UV–vis) was conducted using the DU-800 spectrophotometer (Beckman Coulter, Fullerton, CA, USA) to ascertain the encapsulation of rMOMP.[17] Temperature stability and the morphology of nanoparticles were evaluated using differential scanning calorimetry (DSC), scanning electron microscope (SEM), and atomic force microscopy (AFM).[18,19]

In vitro release of encapsulated-rMOMP

The release of encapsulated-rMOMP was assessed as described.[17,18] Briefly, nanoparticles (100 mg each) were suspended in phosphate-buffered saline (PBS) containing 0.01% sodium azide and incubated at 37 °C. At predetermined time-intervals (up to 31 days), supernatants were collected and stored at −20 °C until quantification of protein.

Stimulation of DCs

Mouse primary-derived bone marrow DCs (Supplementary file) were employed in dose–response, and time-kinetics studies.[2] Cell-free culture supernatants were used to quantify cytokines, and cell pellets for flow cytometry or to extract RNA for TaqMan qPCR studies.

Cytokines quantification

Cytokines (IL-6, IL-12p40, IL-10 and TNF-α) were quantified using Opti-EIA ELISA kits (BD Biosciences, San Jose, CA, USA).[2]

Flow cytometry

Both stimulated and unstimulated DCs were stained with fluorochrome-conjugated antibodies against CD11c, CD40, CD80, CD86, MHC-I, and MHC-II surface receptors as published.[2] Splenocytes (*ex-vivo*) that were collected from immunized mice were pooled per group and labeled with CD3-APC-Cy7, CD4-PerCP-Cy5.5, CD62L-APC, and CD44-PE to quantify memory and effector phenotypes.[2,10] Data were acquired on a LSR II flow

cytometer (BD Bioscience, San Jose, California, USA) with at least 5×10^4 events per sample and analyzed using FCS Express 6 (De Novo Software, Pasadena, CA, USA).

Quantitative PCR

TaqMan qPCR was employed to quantify the transcription levels of chemokines, co-stimulatory molecules, surface binding, and pathogen-sensing receptors.[2] The relative changes in gene expression levels were calculated using $^{\Delta\Delta}$CT, where all values were normalized with respect to the glyceraldehyde 3-phosphate dehydrogenase (GAPDH) "housekeeping" gene mRNA levels.

Immunofluorescence for intracellular trafficking of nanoparticles

Stimulated and unstimulated DCs were probed with antibodies against early endosome (EEA1), late endosome (LE), endoplasmic reticulum (ER), MHC-II and MOMP as reported.[2] Colocalization of organelles with rMOMP was visualized and imaged using a Nikon Eclipse-Ti fluorescence Microscope (Nikon Instruments, Melville, NY, USA).

Mice immunization

Mice were divided into three experimental groups (6 mice/group) as depicted (Supplementary file, Figure S1).[19] Mice in the PLGA-rMOMP group each received three immunizations at two-week intervals with 50 μg/100 μL (subcutaneous) or 50 μg/20 μL (intranasal; 10 μL per nostril) of PLGA-rMOMP in sterile PBS (calculations were based on the actual concentration of rMOMP in nanoparticles). Two-weeks following the last immunization (day 42), mice were sacrificed to collect spleen and serum samples for cellular and antibody analyses, respectively. Mice receiving sterile PBS served as negative controls. The animal studies were performed according to an approved protocol by the Alabama State University's Institutional Animal Care and Use Committee (IACUC).

Serum antibody responses

Serum samples from mice were pooled per group for the detection of rMOMP-specific IgG antibody.[17,19] The end-point titer was considered to be the last sample dilution with readings higher than the mean ± 5 standard deviations of the negative control serum.

Serum-immunoglobulin avidity

Serum samples were used for antigen-specific IgG avidity assessment as published. [10] The percent avidity index (AI) was calculated as:

$$AI\ (\%) = \left[\frac{OD\ with\ urea}{OD\ without\ urea}\right]100$$

In vivo imaging with labeled rMOMP

Mice were each subcutaneously administered 50 μg of infrared-labeled bare rMOMP (rMOMP-IR) or encapsulated-rMOMP-IR (PLGA-rMOMP-IR). An equivalent weight of PLGA-PBS-IR served as the negative control (Supplementary file, Figure S2). All mice were continuously supplied anesthesia (Isoflurane and oxygen blend) using a vaporizer and

monitored employing a live animal imaging system (Analytic Jena, Upland, CA, USA). On day 7, mice were euthanized for collection of sera to quantify rMOMP-specific IgM antibodies.

Statistical Analysis

Data were analyzed by the two-way analysis of variance (ANOVA) followed by the Sidak multiple comparisons using Prism 8 (GraphPad Software, Inc., San Diego, CA, USA). P values ≤0.05 were considered significant.

Results

Physical-structural characterization

Particle size is vital in determining cellular uptake. Thus we employed zeta-sizing to assess PLGA-PBS and PLGA-rMOMP sizes, which were 180 and 182 nm, respectively (Figure 1, A, and B, Table 1). Next, we measured their zeta-potential, a parameter that affects particle stability, and observed −13.2 mV and − 12.6 mV surface charges, respectively, for PLGA-PBS and PLGA-rMOMP (Figure 1, C and D, Table 1), suggesting their stability. The lower polydispersity index (PDI) values of PLGA-PBS (0.135) and PLGA-rMOMP (0.109) were indicative of their closely uniformed nanoparticle sizes (Table 1). Collectively, these findings suggest that the encapsulation of rMOMP did not adversely change the property and size of nanoparticles.

The EE of biomaterials within biodegradable nanoparticles is crucial for the delivery platform since it dictates the concentrations of nanoparticles for immunization studies. Our results showed both high EE (90%) and LC (4.67%) of the encapsulated rMOMP (Table 1). More importantly, the UV-vis spectrum of rMOMP had an optical absorption protein peak at 280 nm that was absent from both PLGA-rMOMP and PLGA-PBS, thereby confirming the encapsulation of rMOMP (Figure 1, E). As shown in Figure 1, F, nanoparticles were thermally stable up to 93 °C, implying that encapsulation caused no adverse effects on the physical properties of PLGA given their observed high thermal stability properties.

AFM analysis depicted the morphology of PLGA-PBS (Figure 1, G and H) and PLGA-rMOMP (Figure 1, I and J) nanoparticles to be round and smooth. Nanoparticles were also in the 100–200 nm size range and smooth as assessed by SEM (Figure 1, K and L), thus corroborating the zeta-sizing and AFM results. Of significance was the sustained slow release of up to 95% of total encapsulated-rMOMP over 31 days (Figure 1, M).

Dose and time-kinetic responses

Previously, we reported that PLGA (85:15) potentiated Th1 immune responses in macrophages as induced by an encapsulated *Chlamydia* peptide.[18] Herein, we investigated PLGA (85:15) potentiating effect of encapsulated-rMOMP in mouse DCs, as they are the primary professional APCs.[20] DCs were stimulated with 0.001, 0.01, 0.1, and 1 μg/mL of either bare rMOMP or PLGA-rMOMP to discern their optimum concentration requirements for cytokines production. Overall, PLGA-rMOMP triggered significantly ($P < 0.0001$) more cytokine secretions than did bare rMOMP at all tested concentrations (Figure 2). We

observed that the differential production of cytokines between PLGA-rMOMP- and bare rMOMP-stimulated DCs were at the 0.1 and 0.01 μg/mL concentrations (Figure 2). The Th1 cytokines, IL-6 (Figure 2, A) and IL-12p40 (Figure 2, C) triggered by bare rMOMP were concentration-dependent in comparison to the slow persistent release of encapsulated-rMOMP from PLGA. Interestingly, PLGA-rMOMP and bare rMOMP dose-dependently induced ($P < 0.0001$) the Th2 cytokine, IL-10 (Figure 2, E), albeit at lower levels. TNF-α was induced by bare rMOMP in a dose-dependent fashion, while PLGA-rMOMP stimulation of TNF-α decreased with increasing stimulant concentrations (Figure 2, G). All cytokines were below the detection levels (4 pg/mL) when DCs were stimulated with 0.001 μg/mL of stimulants or with the PLGA-PBS control (data not shown).

The potentiating effect of PLGA was underscored in time-kinetic experiments using the optimal differential stimulant concentration of 0.01 μg/mL. Both IL-6 (Figure 2, B) and IL-12p40 (Figure 2, D) production commenced as early as 4 h and remained high up to 96 h, whereas IL-10 (Figure 2, F) and TNF-α (Figure 2, H) levels decreased over time. PLGA-PBS did not stimulate cytokine secretions (Figure 2), which confirms PLGA non-stimulatory but potentiating nature. These results suggest that PLGA (85:15) potentiated encapsulated-rMOMP stimulatory capacity by providing its slow and sustained release at low concentrations to trigger higher cytokine production by DCs in contrast to bare rMOMP.

Quantitative PCR

Since our primary goal is to develop an improved *Chlamydia* nanovaccine, the stimulatory strength of PLGA-rMOMP was investigated *via* qPCR for the mRNA transcripts of genes that are required for cellular trafficking and T-cell activation. The mRNA gene transcripts of chemokines (CCL20, CCL7, CXCL2, CCL2, and CXCL1) that are involved in neutrophils, immature DCs, and monocyte trafficking were significantly upregulated ($P < 0.0001$) in PLGA-rMOMP-stimulated DCs as compared to bare rMOMP (Figure 3, A and B). We also observed that PLGA-rMOMP induced significant expression ($P < 0.01$ and $P < 0.05$) of CCL4 and CCL3 that participate in T-cell activation as well as monocyte and immature DCs trafficking (Figure 3, B). CCL8, which triggers Th2 response, was similarly upregulated (Figure 3, B).

We evaluated surface receptor molecules that are essential in innate and adaptive immune responses. Our results showed that PLGA-rMOMP significantly enhanced ($P < 0.0001$, $P < 0.01$ *and* $P < 0.05$) the expression of co-stimulatory molecules (CD40, CD80, and CD86), implying their activation for the subsequent triggering of adaptive immune responses (Figure 3, C). Induced expression of the pathogen-sensing receptor TLR2 by PLGA-rMOMP was seen, suggesting that encapsulated-rMOMP recognition is consistent with its reported TLR2 signaling pathway.[21] PLGA-rMOMP also upregulated the surface binding receptor Fc gamma (FCGR1) that functions in innate and adaptive immunity. Caveolin-1 (CAV1) enhancement, especially on PLGA-rMOMP and PLGA-PBS stimulated DCs, may suggest a role for caveolin-mediated endocytosis in the uptake of nanoparticles (Figure 3, D). PLGA-PBS did not enhance the gene expression of other examined molecules (Figure 3).

Flow cytometry for DCs surface markers

DCs are the main linkers of innate and adaptive immune responses, which drive naive T-cells into specific memory/effector T-cells by antigen presentation through MHC proteins. The process of DCs maturation for an efficient antigen presentation requires the expression of co-stimulatory molecules along with key cytokines and chemokines, as observed herein. We employed flow cytometry to determine the translational expression of the co-stimulatory molecules, CD40, CD80, and CD86, as triggered by stimulants for the activation and maturation of DCs. DCs were stimulated with PLGA-rMOMP, bare rMOMP, or PLGA-PBS and stained with specific fluorochromes-conjugated antibodies. Results as indicated in the upper right quadrants show that PLGA-rMOMP stimulated higher expressions of CD40 (78.32%), CD80 (86.44%) and CD86 (87.07%) (Figure 4, A, D, G) compared to bare rMOMP with CD40 (72.97%), CD80 (79.81%) and CD86 (75.13%) (Figure 4, B, E, H). PLGA-PBS stimulated weak expressions of CD40 (11.73%), CD80 (49.09%) and CD86 (45.28%) (Figure 4, C, F, I) as compared to PLGA-rMOMP or rMOMP.

Next, we evaluated how PLGA-rMOMP would affect the expression levels of MHC-I and MHC-II molecules that are crucial for antigen presentation. PLGA-rMOMP increased the expression of MHC-II (69.35%) relative to rMOMP (48.17%) or PLGA-PBS (37.15%) (Figure 4, J, K, L). Contrastingly, MHC-I expression was weakly induced by PLGA-rMOMP or PLGA-PBS (Figure 4, M, O) as compared to a higher expression induced by rMOMP (Figure 4, N). Our results show that PLGA-rMOMP functionally induced the expression of co-stimulatory and MHC-II molecules for presentation to T-cells.

Intracellular trafficking of nanoparticles

The observation that DCs efficiently endocytosed PLGA-rMOMP nanoparticles prompted further evaluation of their endocytic route for internalization and processing. DCs were exposed to all stimulants, and after 24 h intracellular organelles and MHC-II molecules were labeled with specific antibodies and an anti-MOMP antibody. There was more uptake of PLGA-rMOMP in EEA1 (Figure 5, A) with enhanced colocalization with the released rMOMP, thus confirming rMOMP uptake by DCs and its slow release in comparison to bare rMOMP. Similarly, the colocalization of encapsulated-rMOMP was observed within LE (Figure 5, B) and the ER (Figure 5, C). Expression of MHC-II (Figure 5, D) was enhanced in PLGA-rMOMP-stimulated DCs than those of bare rMOMP, further confirming that PLGA-rMOMP successfully triggered the MHC-II-dependent antigen processing and presentation pathway. PLGA-PBS did not enhance the expression of molecules (Figure 5).

Induction of memory and effector T-cells and antigen-specific serum IgG antibodies

Given that PLGA-rMOMP triggered robust immune responses, we next immunized mice *via* the subcutaneous and intranasal routes to evaluate the effect of immunization routes on the induction of adaptive immune responses. Groups of mice received three subcutaneous or intranasal immunizations with PLGA-rMOMP; the PBS control group only received subcutaneous immunizations (Supplementary file, Figure S1). Splenocytes were pooled per group after sacrifice and stained with labeled antibodies to quantify $CD4^+$ specific memory ($CD44^{high}$ $CD62L^{high}$) and effector ($CD44^{high}$ $CD62L^{low}$) T-cells. Our results showed that mice immunized with PLGA-rMOMP (subcutaneous or intranasal) had elevated $CD3^+CD4^+$

T-cells (Figure 6, C and E) compared to the PBS group (Figure 6, A). Nonetheless, the PLGA-rMOMP subcutaneously immunized mice produced more $CD4^+$ memory (11.61%), and effector (9.71%) T-cells (Figure 6, D) as compared to the intranasal group with fewer $CD4^+$ memory (8.34%) and effector (6.01%) T-cells (Figure 6, F). The PBS group had similar $CD4^+$ memory (7.66%) and effector (6.52%) T-cells (Figure 6, B) as the intranasal group.

The PLGA-rMOMP subcutaneously immunized mice produced an 8-fold higher rMOMP-specific IgG antibody titer (8×10^6) as compared to the intranasally immunized mice (1×10^6). The PBS mice did not produce rMOMP-specific IgG antibodies (Figure 6, G). Notably, mice immunized *via* the subcutaneous route also produced high-avidity functional specific IgG antibodies in comparison to the intranasal mice (Figure 6, H and I). Collectively, the produced cellular and antibody immune responses suggest that the administration route of the nanovaccine may influence the sustained release of the antigen, which is crucial in bolstering adaptive immune responses.

Nanovaccine in vivo tracking

The triggering of adaptive immune responses requires antigen processing *via* DCs and presentation to naïve T-cells for activation and differentiation in lymph nodes. We hypothesized that our nanovaccine would traffic to the nearest lymph nodes of the administration site. Our results showed that the subcutaneous administration of PLGA-rMOMP-IR remained at the site for a longer time (Figure 7, A, D, and G) than the bare rMOMP-IR (Figure 7, B, E, and H) and PLGA-PBS-IR (Figure 7, C, F, and I). The fluorescence intensity of PLGA-rMOMP-IR (Figure 7, J) was strongly visible compared to that of the rMOMP-IR (Figure 7, K), and PLGA-PBS-IR (Figure 7, L) exposed mice. We observed the biodistribution of PLGA-rMOMP-IR in the lymph nodes (cervical, axillary and inguinal) upon opening the peritoneal cavity and scanning of mice on the LI-COR Odyssey imager for better resolution (Figure 7, M). Conversely, only a weak signal intensity of the rMOMP-IR appeared in the popliteal lymph node (Figure 7, N). PLGA-PBS-IR did not traffic to lymph nodes (Figure 7, O). These results suggest that dermal DCs efficiently internalized the PLGA-rMOMP-IR with trafficking to lymph nodes for antigen presentation. Further quantification of rMOMP-specific serum IgM antibodies supports our hypothesis since mice administered the PLGA-rMOMP-IR produced higher IgM antibodies compared to the rMOMP-IR and PLGA-PBS-IR mice (Figure 7, P, Q, and R). These findings confirm the efficient delivery of our nanovaccine *in vivo* for elicitation of the observed adaptive immune responses.

Discussion

Strategies in vaccine designs should consider a delivery vehicle that protects the conformation and degradation of antigens while ensuring their slow and sustained release.[6,10] Biodegradable polymeric nanoparticle-delivery systems have been explored extensively and are attractive for improving the therapeutic values of encapsulated biomolecules.[3,5,22] Indeed, the size range of nanoparticles (100–200 nm) remains critical as it influences the uptake by APCs.[7,23] Encapsulating antigens within polymeric nanoparticles

facilitates their controlled-release, depending on the matrix degradation rate, and also their recognition and uptake by APCs to enhance immune responses.[2,18] The biodegradable polymeric delivery platform provides a novel approach for vaccine designs with or without adjuvants.[11,22] PLGA is a promising delivery system for subunit vaccines due to its safety and proven capacity to increase the efficacy of vaccine candidates.[5,22,24]

Nanotechnology has opened doors to overcome the hurdles of developing efficacious vaccines against *Chlamydia*.[11,17–19,25] It is recognized that many *Chlamydia* vaccine constructs with conventional approaches are still in the pre-clinical developmental stages.[26] Because of that a vaccine strategy based on the employment of targeted antigens and extended-releasing nanoparticles, in all likelihood, maybe an alternative approach that is critical for *Chlamydia* prevention. Previously, we designed a rMOMP-encapsulated PLGA (50:50) nanovaccine formulation that triggered Th1 adaptive immune responses in mice.[17] The extended-release and self-adjuvanting properties of PLGA led[11,24,27,28] us to develop, characterize, and test a new subunit nanovaccine using the slower degrading PLGA (85:15) delivery system for rMOMP.

Here the characterization of our new PLGA-rMOMP revealed that it exhibited all prerequisites criteria as a chlamydial nanovaccine candidate, including a nanometer size, low PDI values, smooth surface, thermal stability, negative zeta-potential, and high EE.[22] These characteristics are an improvement over the larger size and lower EE of the previous PLGA (50:50) formulation.[17] Perhaps the more hydrophobic nature of PLGA (85:15) led to the higher EE and improved LC as reported by other investigators.[29,30] Indeed the characterization properties of our newly designed nanovaccine are in agreement with other PLGA formulations.[17,18,28,31–35]

The potential to trigger immune responses by encapsulated proteins depends on the nanoparticle release pattern.[28] In this study, PLGA-rMOMP had an initial burst releasing ~30% of rMOMP within 24 h and a gradual release up to 31 days accounting for more than 60% of the released rMOMP, which is likely attributable to its high EE or LC as observed by others using the more hydrophobic PLGA.[18,28,36] Although polymeric formulations exhibit an initial burst that can be reduced with the polymer compositions, those exhibiting an initial burst, nonetheless, are still useful in triggering immune response[22,28,37] as confirmed here.

The interaction of PLGA-rMOMP with DCs induced high levels of the Th1 cytokines, IL-6, and IL-12p40 that are essential in defense against chlamydial infections and less of the Th2 cytokine, IL-10, indicating that the continuous slow release of rMOMP predominantly triggered Th1 immune responses.[17,18,38] Evidently, PLGA induces potent Th1 immune responses by delivering encapsulated antigens intracellularly,[39] as supported herein. Also, we observed that PLGA-rMOMP stimulation of IL-10 and TNF-α, but not of IL-6 and IL-12-p40, was concentration-dependent. This dichotomy in the cytokines production dynamics may be attributable to PLGA potentiation of Th1 cytokines, whereby a slow release of the encapsulated-rMOMP stimulates maximal cytokine saturation levels[18] opposite to the dynamic production patterns for IL-10 and TNF-α that probably ensue from the initial burst release. Of support for the observed Th1 and Th2 cytokine production imbalance is that DCs pulsed with rMOMP trigger $CD4^+$ Th1 and not Th2 cytokine

responses *in vitro*.[40] The selective increase of Th1 cytokines, by lower PLGA-rMOMP concentrations may arise from the overall initial burst coupled with the extended-release time. The enhancement of the transcriptional activation of crucial chemokines that play critical roles in the maturation, activation, and differentiation of DCs lend compelling support for the efficient intracellular delivery of rMOMP by PLGA[2,17] to trigger Th1 immune responses.

Activation of adaptive immune responses is a prerequisite for an efficacious vaccine, and the expression of co-stimulatory molecules on DCs is required for T-cell activation.[41] Increased expression of co-stimulatory and MHC-II molecules on DCs underscores the efficient intracellular delivery, processing, and antigen presentation of PLGA-rMOMP. PLGA-rMOMP also upregulated the expression of FCGR1, a potentiator of cellular and humoral immune responses that participates in protective immunity against *Chlamydia* and other intracellular pathogens.[2,42,43] The significance of TLR2 upregulation by PLGA-rMOMP substantiates rMOMP recognition by its putative receptor.[44,45]

It is acknowledged that the hydrophobicity of PLGA nanoparticles increases their uptake by APCs.[46] The intracellular delivery of vaccines by biodegradable nanoparticles *via* the caveolin endocytosis pathway is well-known for the 20–200 nm size range nanoparticles.[2,47] Interestingly, CAV1 was upregulated in DCs by PLGA-rMOMP and PLGA-PBS, which is consistent with its upregulation by a rMOMP peptide encapsulated in PLA–PEG [poly(lactic acid)-poly(ethylene glycol)] nanoparticles.[2] Upregulation of CAV1 by nanoparticles here and previously reported[2] is suggestive of their caveolin-dependent cellular uptake[48] due to their nanometer sizes. Notably, the uptake and endosomal processing of PLGA-rMOMP within DCs strikingly bears a resemblance to the rMOMP peptide encapsulated in PLA–PEG nanoparticles.[2] As such; it seems that rMOMP and its peptide encapsulated in PLA–PEG or PLGA nanoparticles employ a similar trafficking pathway for the induction of immune responses.

The immunogenic potential of vaccines in activating T-cells is critical for the clearance of intracellular pathogens such as *Chlamydia*. A vaccine candidate inducing $CD4^+$ memory T-cells against *Chlamydia* may provide long-lasting immunity.[25,42,49] Stary et al. 2015, elegantly demonstrated that systemic or mucosal immunization of mice with a chlamydial vaccine stimulates memory T-cells; however, only the mucosal route generated effector T-cells.[25] Other investigators have shown that PLA-based co-polymeric nanoparticles are more efficient when administered *via* the subcutaneous route for nanovaccines.[10,18,50] In our study, mice immunized subcutaneously with PLGA-rMOMP generated $CD4^+$ memory ($CD44^{high}$ $CD62L^{high}$) and effector ($CD44^{high}$ $CD62L^{low}$) T-cells, indicating that self-adjuvanting biodegradable polymeric delivery nanocarriers are conducive for this route.[10,17] Contrastingly, the intranasal route only enhanced $CD4^+$ T-cells but not memory ($CD44^{high}$ $CD62L^{high}$) and effector ($CD44^{high}$ $CD62L^{low}$) T-cells phenotypes, perhaps suggesting that this route may require an adjuvant to enhance its efficiency.[25,51]

The humoral immune response plays a pivotal role in preventing the spread of infection and antibodies produced during a chlamydial infection contribute to protective immunity.[52] Here PLGA-rMOMP subcutaneously immunized mice produced higher levels of rMOMP-

specific antibodies in comparison to the intranasal mice, further underscoring that systemic immunization induces chlamydial antigen-specific IgG antibodies.[17] Despite the increased production of antibodies against an antigen, functionality reflects maintaining long-term humoral memory responses.[10,53] Lack of functional antibodies has an impact on reducing the vaccine's efficacy.[54] In the current study, the subcutaneous route provided highly functional antibodies in contrast to the mucosal route.

Overall, the immune responses triggered by PLGA-rMOMP indicate the involvement of lymph nodes. The visual confirmation from the live imaging uptake of the nanovaccine with a high signal intensity in lymph nodes is proof of concept that PLGA-rMOMP is a compatible and immunogenic formulation.[7] Worthy of mention is that the labeling of rMOMP with the IR dye did not compromise its integrity as confirmed by the production of IgM in mice injected with the PLGA-rMOMP-IR. Reportedly, PLGA can be formulated to target lymph nodes specifically.[55,56] Although bare rMOMP-IR was observed adjacent to the popliteal lymph node with a low signal intensity, the absence of IgM production in mice suggests that our PLGA (85:15) nanocarrier delivery system plays a crucial role in the induction of antibodies.

Predicting nanoparticles behavior is a complex issue in animal models, especially when it pertains to intracellular pathogens. PLGA nanoparticles are gaining attention as vaccine delivery systems for intracellular pathogens,[5,17,36,57] though they may be hydrolyzed at mucosal surfaces. Nevertheless, coating their surface with a glycol or chitosan can control this problem.[58,59] Hamdy et al. 2011, described the relationship between systemic immunization and activation of DCs, which may become more robust with an adjuvant,[7,60] particularly for the mucosal route. The present study employed the self-adjuvanting PLGA (85:15) nanoparticles for the extended-release of chlamydial rMOMP for intracellular processing and presentation by DCs[20] to induce immune responses. Our data disclose that the PLGA-rMOMP (85:15) nanovaccine enhanced the activation of DCs and augmented *Chlamydia*-specific rMOMP $CD4^+$ memory, and effector T-cells and antibody adaptive immune responses in immunized mice. This alternative approach in the development of a chlamydial rMOMP nanovaccine using an extended-releasing biodegradable-polymeric nanoparticle delivery platform is worthy of future efficacy testing.

Supplementary Material

Refer to Web version on PubMed Central for supplementary material.

Acknowledgments

The authors would like to thank Yvonne Williams, LaShaundria Lucas, and Juwana Smith-Henderson of CNBR for their excellent administrative assistance. Special thanks go to Marion L. Spell, the University of Alabama at Birmingham, CFAR Flow Core Facility (An NIH funded program-P30 AI027767), for assistance with the FACS data acquisition. G. H. G. is a member of the Research Career of CONICET (Argentina).

Funding source:

This research was supported by the National Institute of Allergy and Infectious Diseases of the National Institutes of Health under Award Number R21AI111159, NIH-NIGMS-RISE (2R25GM106995-06A1) and the National Science Foundation (NSF)-CREST (HRD-1241701) and NSF-HBCU-RISE (HRD-1646729) grants. The content of

this study is solely the responsibility of the authors and does not necessarily represent the official views of the National Institutes of Health.

Abbreviations:

DCs	Dendritic cells
MOMP	Major outer membrane protein
rMOMP	Recombinant major outer membrane protein
EE	Encapsulation efficiency
APCs	Antigen-presenting cells
LC	Loading capacity
UV–vis	Ultraviolet visualizations
PDI	Polydispersity index
SEM	Scanning electron microscope
AFM	Atomic force microscopy
DSC	Differential scanning calorimetry
qPCR	Quantitative polymerase chain reaction
GAPDH	Glyceraldehyde 3-phosphate dehydrogenase
TLR	Toll-like receptor
MHC	Major histocompatibility Complex
DAPI	2-(4-amidinophenyl)-6-indolecarbamidine dihydrochloride
AI	Avidity Index
ANOVA	Analysis of variance
CAV1	Caveolin-1
PBS	Phosphate buffered saline
FCGR1	Fc gamma receptor
EEA1	Early endosomes
LE	Late endosomes
ER	Endoplasmic reticulum

References

1. Skwarczynski M, Zaman M, Toth I. Lipo-peptides/saccharides for peptide vaccine delivery. In: Kastin AJ, editor. Handbook of Biologically Active Peptides. Boston: Academic Press; 2013. p. 571–9.
2. Dixit S, Sahu R, Verma R, Duncan S, Giambartolomei GH, Singh SR, et al. Caveolin-mediated endocytosis of the -*Chlamydia* M278 outer membrane peptide encapsulated in poly(lactic acid)-poly(ethylene glycol) nanoparticles by mouse primary dendritic cells enhances specific immune effectors mediated by MHC class II and CD4(+) T cells. Biomaterials 2018;159:130–45. [PubMed: 29324305]
3. Zhao L, Seth A, Wibowo N, Zhao CX, Mitter N, Yu C, et al. Nanoparticle vaccines. Vaccine 2014;32:327–37. [PubMed: 24295808]
4. Sun X, Xu C, Wu G, Ye Q, Wang C. Poly(lactic-co-glycolic acid): applications and future prospects for periodontal tissue regeneration. Polymers (Basel) 2017;9.
5. Allahyari M, Mohit E. Peptide/protein vaccine delivery system based on PLGA particles. Hum Vaccin Immunother 2016;12:806–28. [PubMed: 26513024]
6. Bachmann MF, Jennings GT. Vaccine delivery: a matter of size, geometry, kinetics and molecular patterns. Nat Rev Immunol 2010;10:787–96. [PubMed: 20948547]
7. Silva AL, Soema PC, Slutter B, Ossendorp F, Jiskoot W. PLGA particulate delivery systems for subunit vaccines: linking particle properties to immunogenicity. Hum Vaccin Immunother 2016;12:1056–69. [PubMed: 26752261]
8. Sneh-Edri H, Likhtenshtein D, Stepensky D. Intracellular targeting of PLGA nanoparticles encapsulating antigenic peptide to the endoplasmic reticulum of dendritic cells and its effect on antigen cross-presentation in vitro. Mol Pharm 2011;8:1266–75. [PubMed: 21661745]
9. Rosalia RA, Cruz LJ, van Duikeren S, Tromp AT, Silva AL, Jiskoot W, et al. CD40-targeted dendritic cell delivery of PLGA-nanoparticle vaccines induce potent anti-tumor responses. Biomaterials 2015;40:88–97. [PubMed: 25465442]
10. Verma R, Sahu R, Dixit S, Duncan SA, Giambartolomei GH, Singh SR, et al. The *Chlamydia* M278 major outer membrane peptide encapsulated in the poly(lactic acid)-poly(ethylene glycol) nanoparticulate self-adjuvanting delivery system protects mice against a *Chlamydia muridarum* genital tract challenge by stimulating robust systemic and local mucosal immune responses. Front Immunol 2018;9:2369. [PubMed: 30374357]
11. Sahu R, Verma R, Dixit S, Igietseme JU, Black CM, Duncan S, et al. Future of human *Chlamydia* vaccine: potential of self-adjuvanting biodegradable nanoparticles as safe vaccine delivery vehicles. Expert Rev Vaccines 2018;17:217–27. [PubMed: 29382248]
12. Poston TB, Darville T. *Chlamydia trachomatis*: protective adaptive responses and prospects for a vaccine. Curr Top Microbiol Immunol 2018;412:217–37. [PubMed: 27033698]
13. Hoenderboom BM, van Benthem BHB, van Bergen J, Dukers-Muijrers N, Gotz HM, Hoebe C, et al. Relation between *Chlamydia trachomatis* infection and pelvic inflammatory disease, ectopic pregnancy and tubal factor infertility in a Dutch cohort of women previously tested for *Chlamydia* in a *Chlamydia* screening trial. Sex Transm Infect 2019;95:300–6. [PubMed: 30606817]
14. Mpiima DP, Wasswa Salongo G, Lugobe H, Ssemujju A, Mumbere Mulisya O, Masinda A, et al. Association between prior *Chlamydia* trachomatis infection and ectopic pregnancy at a tertiary care hospital in South Western Uganda. Obstet Gynecol Int 2018;2018:4827353. [PubMed: 29686708]
15. Yu H, Karunakaran KP, Jiang X, Brunham RC. Subunit vaccines for the prevention of mucosal infection with *Chlamydia* trachomatis. Expert Rev Vaccines 2016;15:977–88. [PubMed: 26938202]
16. Southern T, Bess L, Harmon J, Taylor L, Caldwell H. Fluorometric high-throughput assay for measuring chlamydial neutralizing antibody. Clin Vaccine Immunol 2012;19:1864–9. [PubMed: 23015646]
17. Fairley SJ, Singh SR, Yilma AN, Waffo AB, Subbarayan P, Dixit S, et al. *Chlamydia trachomatis* recombinant MOMP encapsulated in PLGA nanoparticles triggers primarily T helper 1 cellular

and antibody immune responses in mice: a desirable candidate nanovaccine. Int J Nanomedicine 2013;8:2085–99. [PubMed: 23785233]

18. Taha MA, Singh SR, Dennis VA. Biodegradable PLGA85/15 nanoparticles as a delivery vehicle for *Chlamydia trachomatis* recombinant MOMP-187 peptide. Nanotechnology 2012;23:325101. [PubMed: 22824940]
19. Dixit S, Singh SR, Yilma AN, Agee RD 2nd, Taha M, Dennis VA. Poly (lactic acid)-poly(ethylene glycol) nanoparticles provide sustained delivery of a *Chlamydia trachomatis* recombinant MOMP peptide and potentiate systemic adaptive immune responses in mice. Nanomedicine 2014;10:1311–21. [PubMed: 24602605]
20. Tonigold M, Mailander V. Endocytosis and intracellular processing of nanoparticles in dendritic cells: routes to effective immunonanomedicines. Nanomedicine (Lond) 2016;11:2625–30. [PubMed: 27628644]
21. Cheng C, Pal S, Tifrea D, Jia Z, de la Maza LM. A vaccine formulated with a combination of TLR-2 and TLR-9 adjuvants and the recombinant major outer membrane protein elicits a robust immune response and significant protection against a *Chlamydia muridarum* challenge. Microbes Infect 2014;16:244–52. [PubMed: 24291713]
22. Pati R, Shevtsov M, Sonawane A. Nanoparticle vaccines against infectious diseases. Front Immunol 2018;9:2224. [PubMed: 30337923]
23. Howard GP, Verma G, Ke X, Thayer WM, Hamerly T, Baxter VK, et al. Critical size limit of biodegradable nanoparticles for enhanced lymph node trafficking and paracortex penetration. Nano Research 2019;12:837–44. [PubMed: 33343832]
24. Makadia HK, Siegel SJ. Poly lactic-co-glycolic acid (PLGA) as biodegradable controlled drug delivery carrier. Polymers (Basel) 2011;3:1377–97. [PubMed: 22577513]
25. Stary G, Olive A, Radovic-Moreno AF, Gondek D, Alvarez D, Basto PA, et al. VACCINES. A mucosal vaccine against *Chlamydia trachomatis* generates two waves of protective memory T cells. Science 2015;348aaa8205.
26. Poston TB, Gottlieb SL, Darville T. Status of vaccine research and development of vaccines for *Chlamydia trachomatis* infection. Vaccine 2019;37:7289–94. [PubMed: 28111145]
27. Salari F, Varasteh AR, Vahedi F, Hashemi M, Sankian M. Down-regulation of Th2 immune responses by sublingual administration of poly (lactic-co-glycolic) acid (PLGA)-encapsulated allergen in BALB/c mice. Int Immunopharmacol 2015;29:672–8. [PubMed: 26404189]
28. Singh D, Somani VK, Aggarwal S, Bhatnagar R. PLGA (85:15) nanoparticle based delivery of rL7/L12 ribosomal protein in mice protects against *Brucella abortus* 544 infection: a promising alternate to traditional adjuvants. Mol Immunol 2015;68:272–9. [PubMed: 26442664]
29. Kabiri M, Sankian M, Sadri K, Tafaghodi M. Robust mucosal and systemic responses against HTLV-1 by delivery of multi-epitope vaccine in PLGA nanoparticles. Eur J Pharm Biopharm 2018;133:321–30. [PubMed: 30408519]
30. Mukherjee B, Santra K, Pattnaik G, Ghosh S. Preparation, characterization and in-vitro evaluation of sustained release protein-loaded nanoparticles based on biodegradable polymers. Int J Nanomedicine 2008;3:487–96. [PubMed: 19337417]
31. Muhamad N, Plengsuriyakarn T, Chittasupho C, Na-Bangchang K. The potential of atractylodin-loaded PLGA nanoparticles as chemotherapeutic for cholangiocarcinoma. Asian Pac J Cancer Prev 2020;21:935–41. [PubMed: 32334453]
32. Gao M, Long X, Du J, Teng M, Zhang W, Wang Y, et al. Enhanced curcumin solubility and antibacterial activity by encapsulation in PLGA oily core nanocapsules. Food Funct 2020;11:448–55. [PubMed: 31829367]
33. Dollo G, Boucaud Y, Amela-Cortes M, Molard Y, Cordier S, Brandhonneur N. PLGA nanoparticles embedding molybdenum cluster salts: influence of chemical composition on physico-chemical properties, encapsulation efficiencies, colloidal stabilities and in vitro release. Int J Pharm 2020;576:119025. [PubMed: 31926277]
34. Streck S, Neumann H, Nielsen HM, Rades T, McDowell A. Comparison of bulk and microfluidics methods for the formulation of poly-lactic-co-glycolic acid (PLGA) nanoparticles modified with cell-penetrating peptides of different architectures. Int J Pharm X 2019;1:100030. [PubMed: 31517295]

35. Manish M, Rahi A, Kaur M, Bhatnagar R, Singh S. A single-dose PLGA encapsulated protective antigen domain 4 nanoformulation protects mice against *Bacillus anthracis* spore challenge. PLoS One 2013;8e61885.
36. Singh D, Goel D, Bhatnagar R. Recombinant L7/L12 protein entrapping PLGA (poly lactide-co-glycolide) micro particles protect BALB/c mice against the virulent *B. abortus* 544 infection. Vaccine 2015;33:2786–92. [PubMed: 25930114]
37. Yeo Y, Park K. Control of encapsulation efficiency and initial burst in polymeric microparticle systems. Arch Pharm Res 2004;27:1–12. [PubMed: 14969330]
38. Williams DM, Grubbs BG, Darville T, Kelly K, Rank RG. A role for interleukin-6 in host defense against murine *Chlamydia trachomatis* infection. Infect Immun 1998;66:4564–7. [PubMed: 9712822]
39. Li P, Asokanathan C, Liu F, Khaing KK, Kmiec D, Wei X, et al. PLGA nano/micro particles encapsulated with pertussis toxoid (PTd) enhances Th1/Th17 immune response in a murine model. Int J Pharm 2016;513:183–90. [PubMed: 27586408]
40. Shaw J, Grund V, Durling L, Crane D, Caldwell HD. Dendritic cells pulsed with a recombinant chlamydial major outer membrane protein antigen elicit a CD4(+) type 2 rather than type 1 immune response that is not protective. Infect Immun 2002;70:1097–105. [PubMed: 11854188]
41. Fujii S, Liu K, Smith C, Bonito AJ, Steinman RM. The linkage of innate to adaptive immunity via maturing dendritic cells in vivo requires CD40 ligation in addition to antigen presentation and CD80/86 costimulation. J Exp Med 2004;199:1607–18. [PubMed: 15197224]
42. Moore T, Ekworomadu CO, Eko FO, MacMillan L, Ramey K, Ananaba GA, et al. Fc receptor-mediated antibody regulation of T cell immunity against intracellular pathogens. J Infect Dis 2003;188:617–24. [PubMed: 12898452]
43. Moore T, Ananaba GA, Bolier J, Bowers S, Belay T, Eko FO, et al. Fc receptor regulation of protective immunity against *Chlamydia trachomatis*. Immunology 2002;105:213–21. [PubMed: 11872097]
44. O'Connell CM, Ionova IA, Quayle AJ, Visintin A, Ingalls RR. Localization of TLR2 and MyD88 to *Chlamydia trachomatis* inclusions. Evidence for signaling by intracellular TLR2 during infection with an obligate intracellular pathogen. J Biol Chem 2006;281:1652–9. [PubMed: 16293622]
45. Poikonen K, Lajunen T, Silvennoinen-Kassinen S, Leinonen M, Saikku P. Effects of CD14, TLR2, TLR4, LPB, and IL-6 gene polymorphisms on *Chlamydia pneumoniae* growth in human macrophages in vitro. Scand J Immunol 2009;70:34–9. [PubMed: 19522765]
46. Foged C, Brodin B, Frokjaer S, Sundblad A. Particle size and surface charge affect particle uptake by human dendritic cells in an in vitro model. Int J Pharm 2005;298:315–22. [PubMed: 15961266]
47. Sahin A, Esendagli G, Yerlikaya F, Caban-Toktas S, Yoyen-Ermis D, Horzum U, et al. A small variation in average particle size of PLGA nanoparticles prepared by nanoprecipitation leads to considerable change in nanoparticles' characteristics and efficacy of intracellular delivery. Artif Cells Nanomed Biotechnol 2017;45:1657–64. [PubMed: 28084837]
48. Zhang L, Xu Y, Cao W, Xie S, Wen L, Chen G. Understanding the translocation mechanism of PLGA nanoparticles across round window membrane into the inner ear: a guideline for inner ear drug delivery based on nanomedicine. Int J Nanomedicine 2018;13:479–92. [PubMed: 29403277]
49. Sallusto F, Lanzavecchia A, Araki K, Ahmed R. From vaccines to memory and back. Immunity 2010;33:451–63. [PubMed: 21029957]
50. Cappellano G, Woldetsadik AD, Orilieri E, Shivakumar Y, Rizzi M, Carniato F, et al. Subcutaneous inverse vaccination with PLGA particles loaded with a MOG peptide and IL-10 decreases the severity of experimental autoimmune encephalomyelitis. Vaccine 2014;32:5681–9. [PubMed: 25149432]
51. Clements JD, Norton EB. The mucosal vaccine adjuvant LT(R192G/L211A) or dmLT. mSphere 2018;3.
52. Picard MD, Cohane KP, Gierahn TM, Higgins DE, Flechtner JB. High-throughput proteomic screening identifies *Chlamydia trachomatis* antigens that are capable of eliciting T cell and antibody responses that provide protection against vaginal challenge. Vaccine 2012;30:4387–93. [PubMed: 22682294]

53. Alam MM, Arifuzzaman M, Ahmad SM, Hosen MI, Rahman MA, Rashu R, et al. Study of avidity of antigen-specific antibody as a means of understanding development of long-term immunological memory after *Vibrio cholerae* O1 infection. Clin Vaccine Immunol 2013;20:17–23. [PubMed: 23114701]

54. Pannuti CS, Morello RJ, Moraes JC, Curti SP, Afonso AM, Camargo MC, et al. Identification of primary and secondary measles vaccine failures by measurement of immunoglobulin G avidity in measles cases during the 1997 Sao Paulo epidemic. Clin Diagn Lab Immunol 2004;11:119–22. [PubMed: 14715557]

55. Rao DA, Forrest ML, Alani AW, Kwon GS, Robinson JR. Biodegradable PLGA based nanoparticles for sustained regional lymphatic drug delivery. J Pharm Sci 2010;99:2018–31. [PubMed: 19902520]

56. Subramanian S, Pandey U, Gugulothu D, Patravale V, Samuel G. Modification of PLGA nanoparticles for improved properties as a 99mTc-labeled agent in sentinel lymph node detection. Cancer Biother Radiopharm 2013;28:598–606. [PubMed: 23705864]

57. Chong CS, Cao M, Wong WW, Fischer KP, Addison WR, Kwon GS, et al. Enhancement of T helper type 1 immune responses against hepatitis B virus core antigen by PLGA nanoparticle vaccine delivery. J Control Release 2005;102:85–99. [PubMed: 15653136]

58. Pawar D, Mangal S, Goswami R, Jaganathan KS. Development and characterization of surface modified PLGA nanoparticles for nasal vaccine delivery: effect of mucoadhesive coating on antigen uptake and immune adjuvant activity. Eur J Pharm Biopharm 2013;85:550–9. [PubMed: 23831265]

59. O'Hagan DT, Singh M, Ulmer JB. Microparticle-based technologies for vaccines. Methods 2006;40:10–9. [PubMed: 16997709]

60. Hamdy S, Haddadi A, Hung RW, Lavasanifar A. Targeting dendritic cells with nano-particulate PLGA cancer vaccine formulations. Adv Drug Deliv Rev 2011;63:943–55. [PubMed: 21679733]

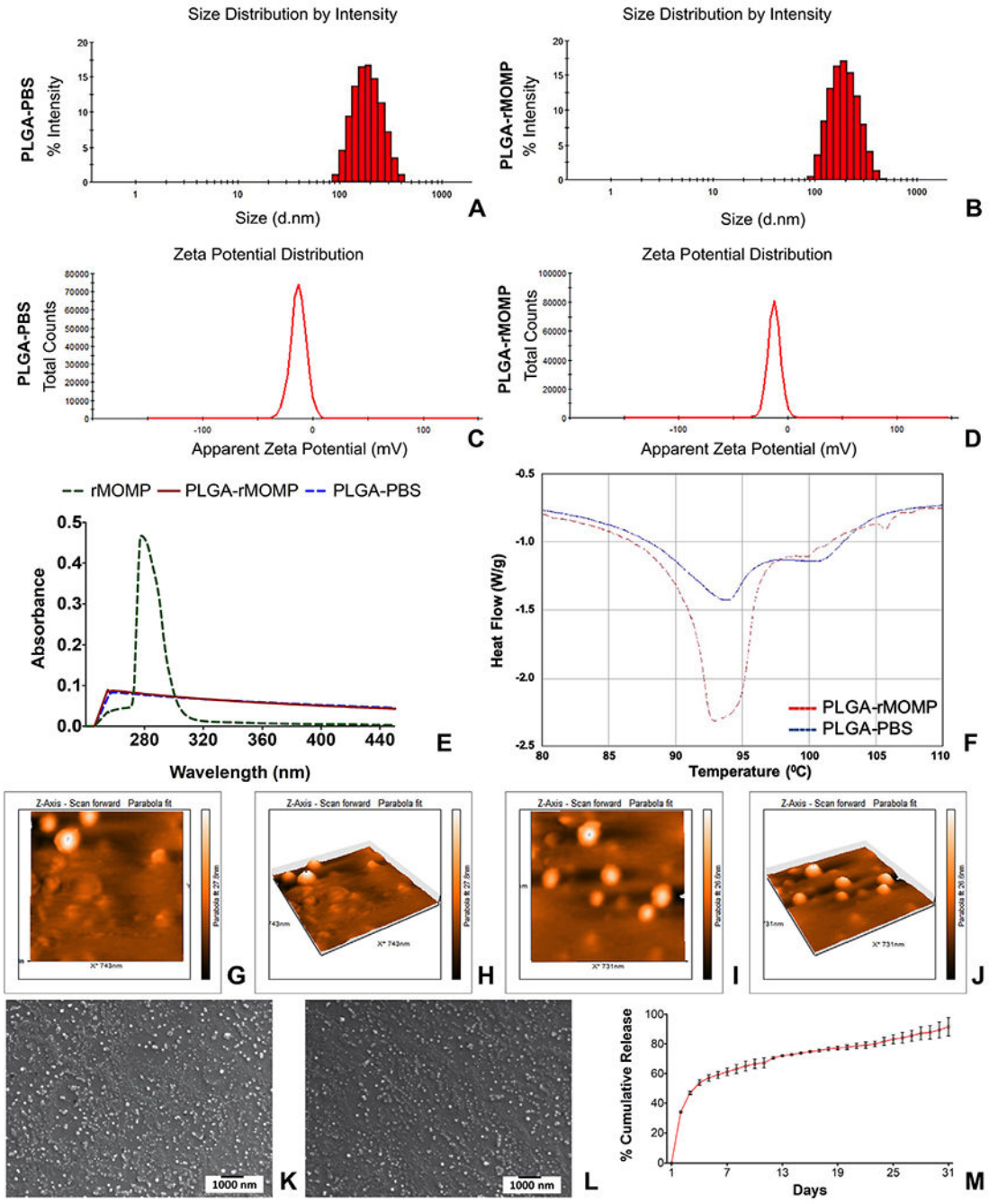

Figure 1.

Physical-structural characterization. Analyses of the zeta-sizing (A, B), and zeta-potential (C, D), UV-vis (E), DSC (F), AFM of PLGA-PBS at two-dimension (G) and three-dimension (H); PLGA-rMOMP at two-dimension (I) and three-dimension (J), PLGA-PBS (K), and PLGA-rMOMP (L) and *in vitro* release of rMOMP (M).

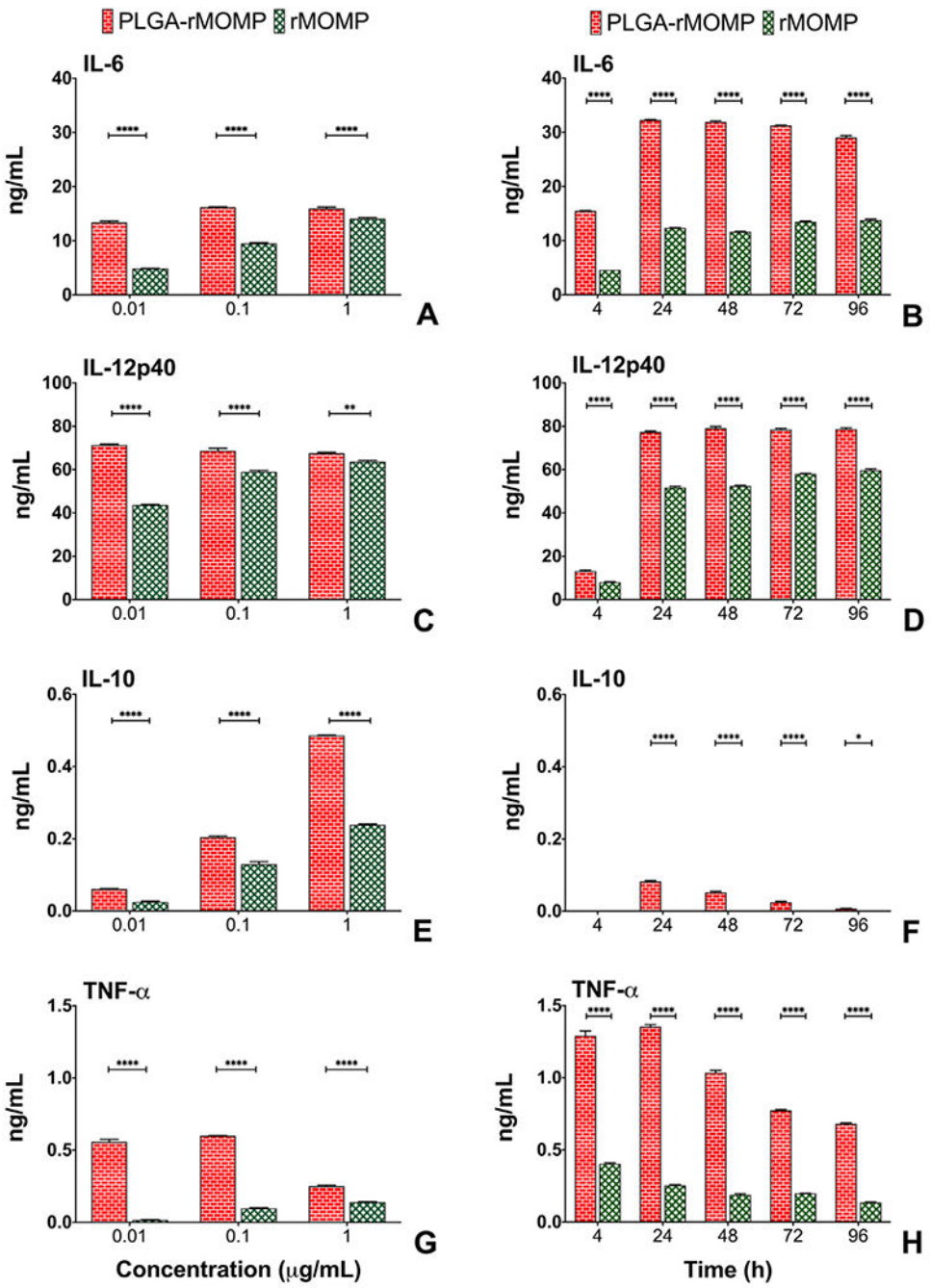

Figure 2.

Secretion of cytokines induced by stimulated DCs. DCs were exposed to various concentrations (0.01, 0.1 and 1 μg/mL) of bare rMOMP or PLGA-rMOMP or an equivalent weight of PLGA-PBS. Cell-free supernatants were collected at 24 h, and quantifications of IL-6 (A), IL-12p40 (C), IL-10 (E), and TNF-α (G) were performed using cytokine-specific ELISAs. Cumulative production of cytokines was determined after exposing DCs to 0.01 μg/mL of bare rMOMP or PLGA-rMOMP. Cell-free supernatants were collected at 4, 24, 48, 72, and 96 h time-points to quantify IL-6 (B), IL-12p40 (D), IL-10 (F), and TNF-α

(H). Each bar represents the mean ± standard deviation of triplicate samples. Experiments were repeated at least three times. Significance between groups was established at ****$P <$ 0.0001 **$P < 0.01$ and *$P < 0.05$.

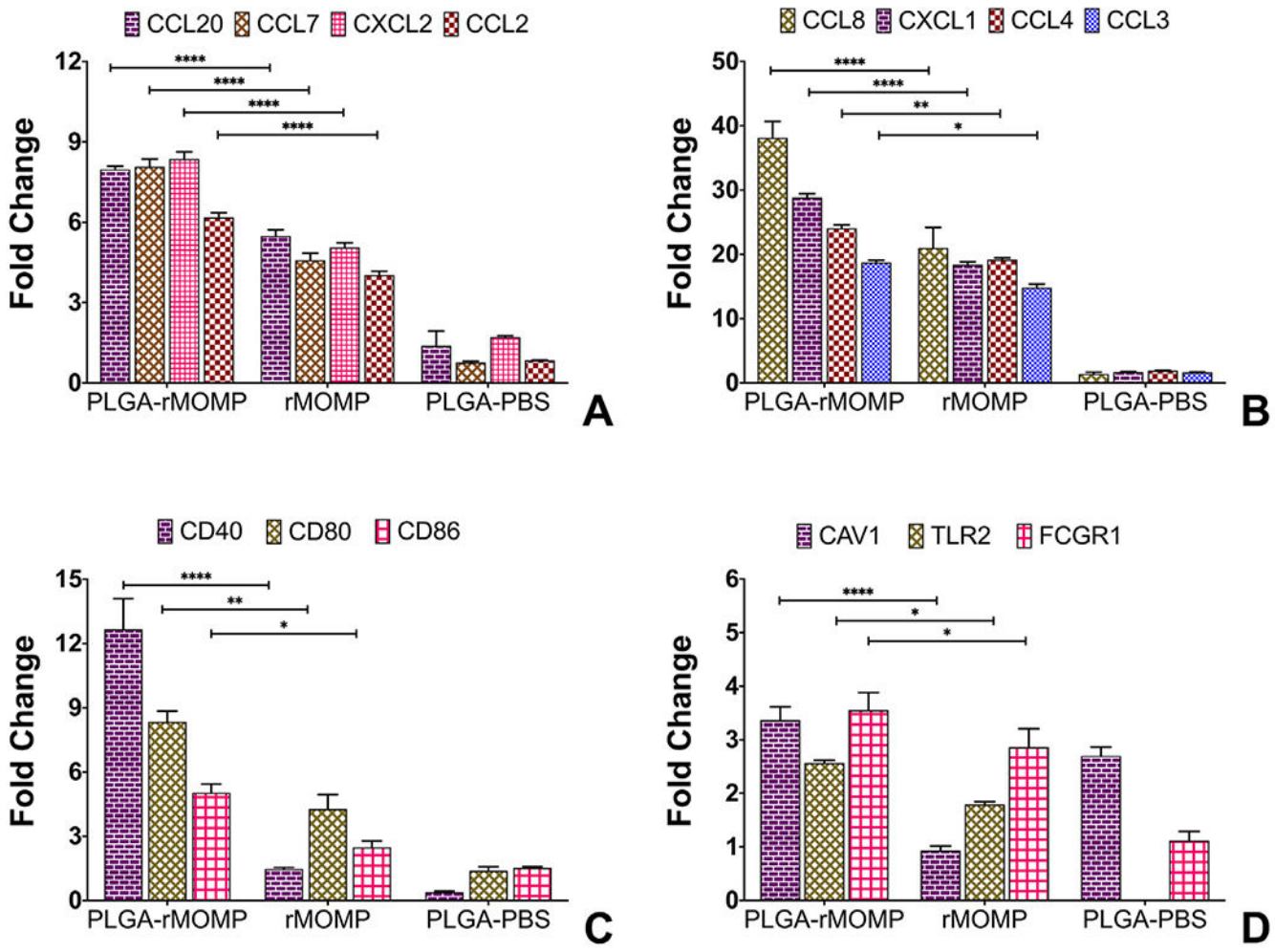

Figure 3.

Differential transcriptional expression of chemokines and cell surface receptors. DCs were stimulated for 24 h with 0.01 μg of PLGA-rMOMP or bare rMOMP or an equivalent weight of PLGA-PBS. TaqMan gene expression assay probes were employed to quantify the expression of chemokines and receptors mRNA gene transcripts. Each bar represents the mean ± standard deviation of triplicate samples. Experiments were repeated at least three times. Significance between groups was established at ****$P < 0.0001$ and **$P < 0.01$ and *$P < 0.05$.

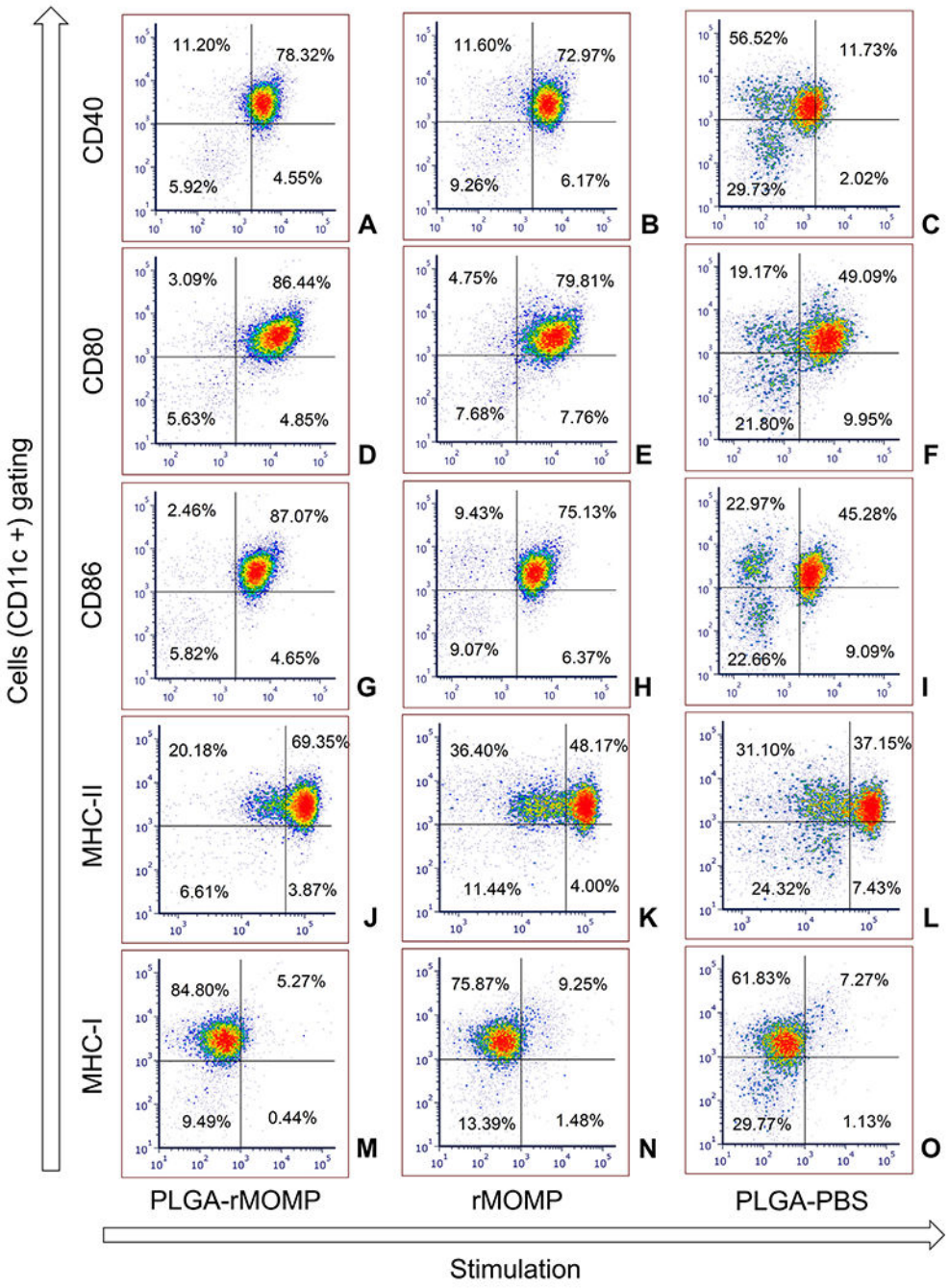

Figure 4.

Enhanced expression of co-stimulatory and MHC molecules. DCs were stimulated with 0.01 μg of PLGA-rMOMP or bare rMOMP for 24 h and stained with fluorochrome-conjugated antibodies. Stained cells were subjected to flow cytometric analysis of surface molecules by gating on $CD11c^+$ cells, CD40 (A-C), CD80 (D-F), CD86 (G-I), MHC-II (J-L) and MHC-I (M-O). PLGA-PBS was used as a negative control. The upper right quadrants are % positive cells for the respective expression of surface molecules. Experiments were repeated at least three times.

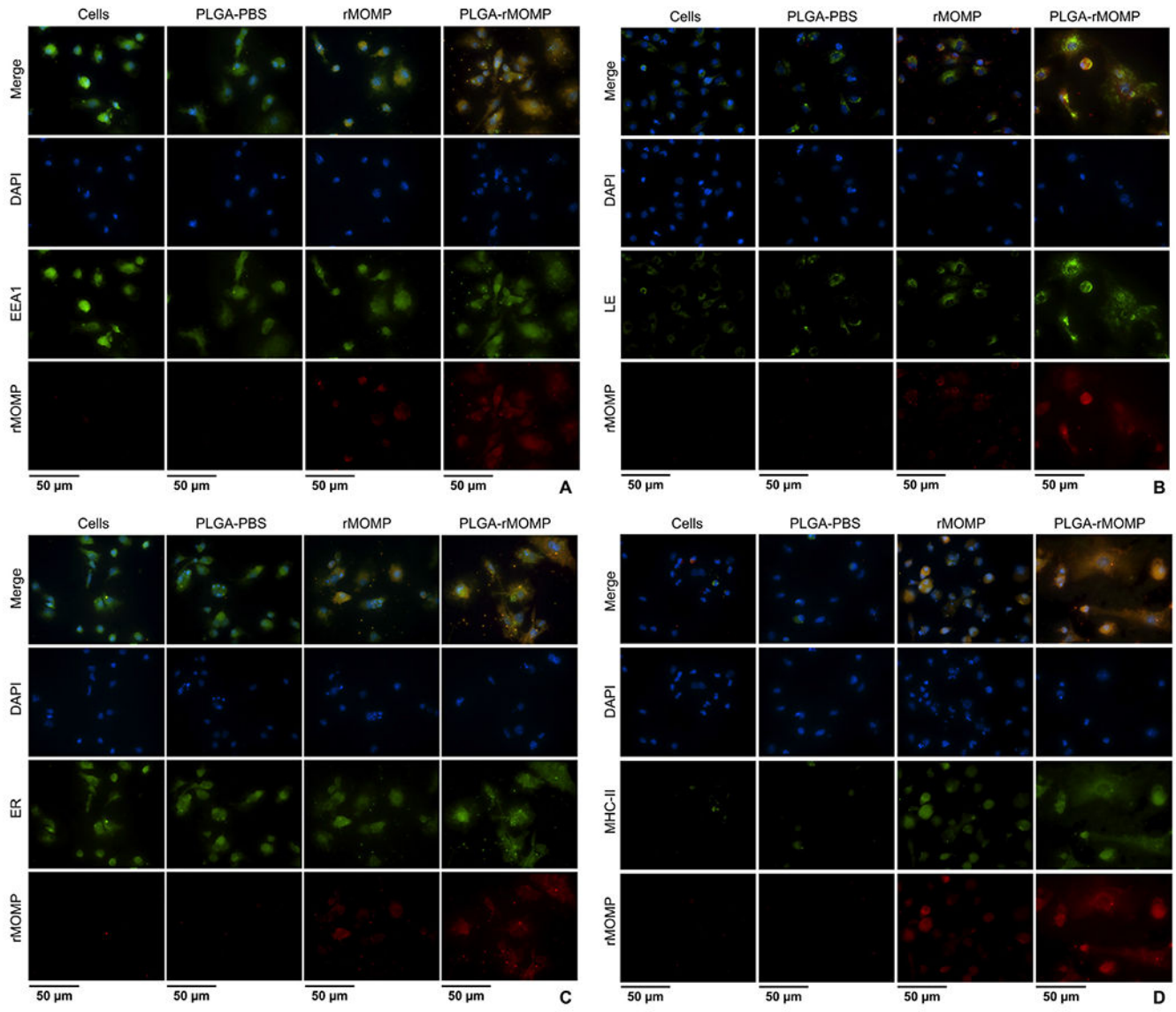

Figure 5.

Intracellular trafficking and colocalization of the released rMOMP in DCs. DCs were stimulated with 0.01 μg of PLGA-rMOMP or bare rMOMP for 24 h. Cells were stained for subcellular organelles (green), including early endosomes (EEA1) (A), late endosomes (LE) (B), endoplasmic reticulum (ER) (C) and major histocompatibility complex-II (MHC-II) (D). Colocalization was confirmed by probing for rMOMP (red) in DCs. DAPI (blue) was used as nuclei stain. The top row (merge) indicates the overlay of images. Direct visualization and imaging were performed by employing immunofluorescence microscopy. Experiments were repeated at least two times.

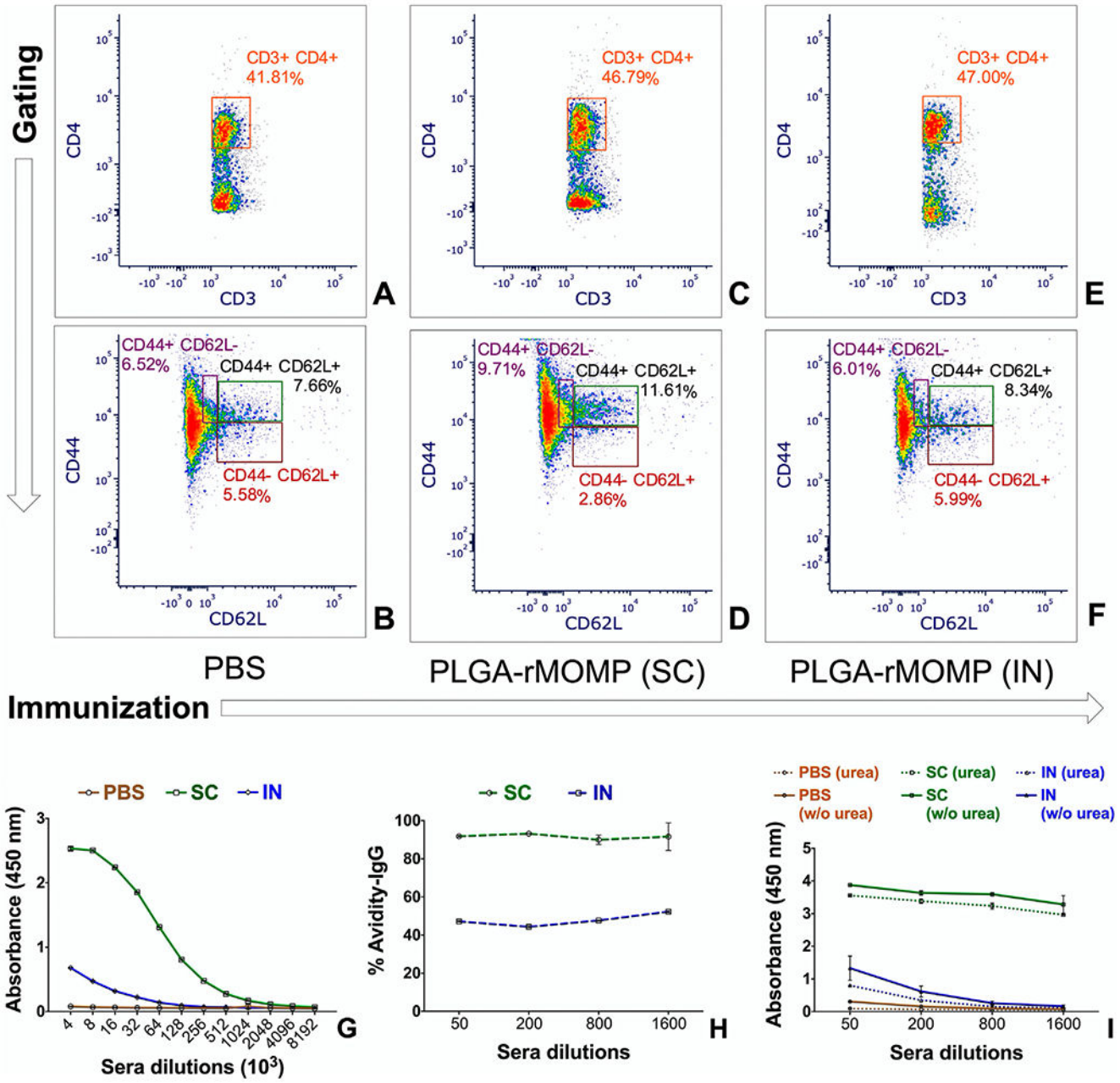

Figure 6.

Chlamydia-specific memory and effector T-cells and antibody responses. Mice were immunized with 50 μg of PLGA-rMOMP (subcutaneous or intranasal) three times at two-week intervals and sacrificed two-weeks after the third immunization. Splenocytes were isolated and stained with fluorochrome-conjugated antibodies; anti-CD3-APC-Cy7, anti-CD4-PerCP-Cy5.5, anti-CD62L-APC, and anti-CD44-PE. Stained splenocytes were subjected to flow cytometry analysis by gating on $CD3^+$ cells to quantify $CD3^+CD4^+$ derived memory ($CD44^+CD62L^+$) and effector ($CD44^+CD62L^-$) phenotypes of T-cells for the PBS (A, B), subcutaneous (SC) PLGA-rMOMP (C, D) and intranasal (IN) PLGA-rMOMP (E, F) immunized groups. Sera collected and pooled per group of mice were diluted

at a two-fold serial dilution to determine the end-point rMOMP-specific IgG antibody titers via ELISA (G). Avidity index of rMOMP-specific IgG antibodies was determined at lower sera dilutions using ELISA. Percent (%) avidity index (H); avidity absorbance values (I). Sera samples were run in triplicates, and experiments were repeated at least three times.

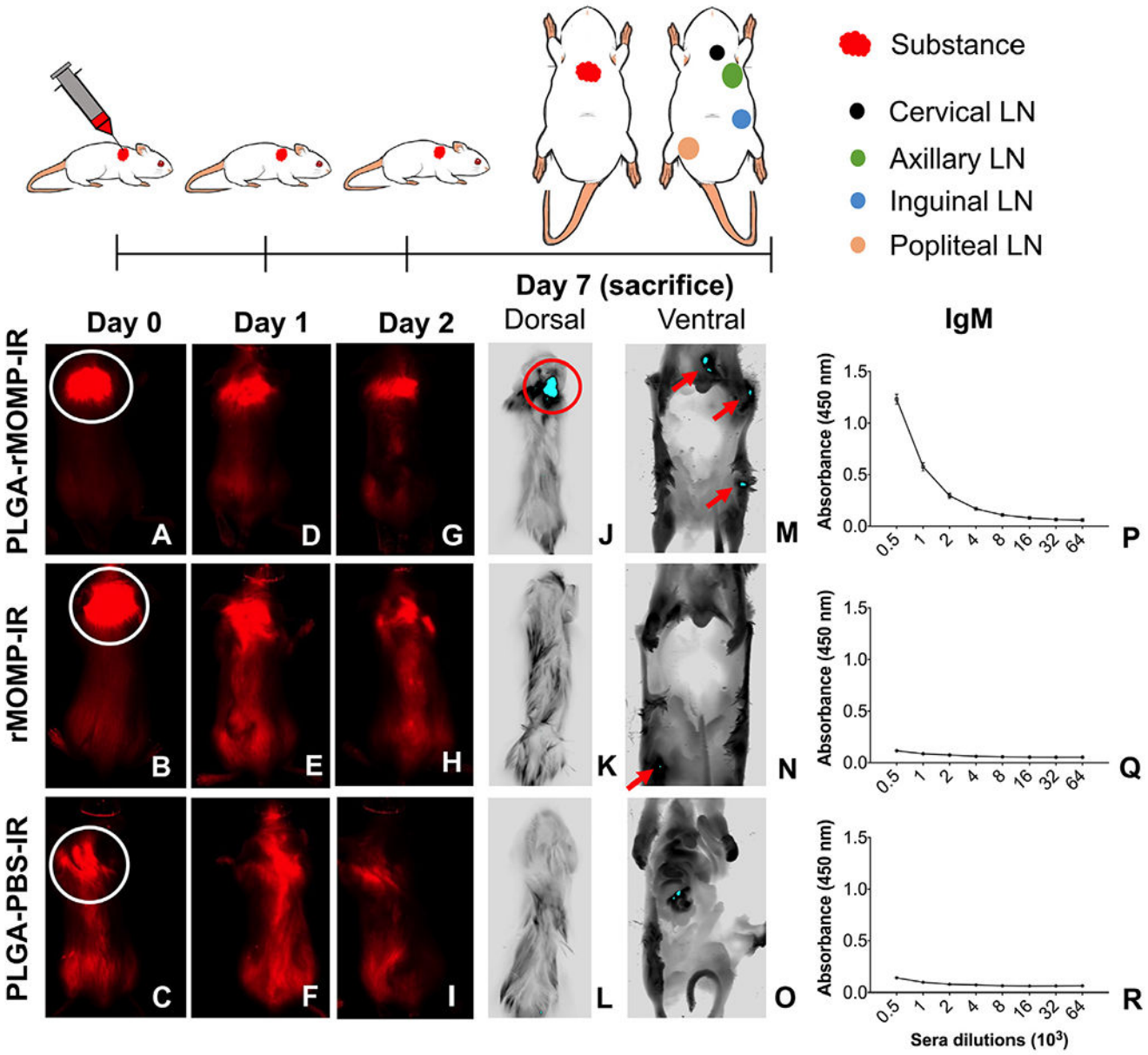

Figure 7.

In vivo tracking of nanoparticles uptake in BALB/c mice. Mice were administered rMOMP-IR, PLGA-rMOMP-IR, or PLGA-PBS-IR once *via* the subcutaneous route (shown in white circles). Images of mice were acquired using a live animal imaging system on day 0 (A, B, C), day 1 (D, E, F), day 2 (G, H, I), followed by sacrificed on day 7. Dorsal images (J, K, L) were taken on day 7 to locate the fluorescence signals at the administration site. Mice were opened and imaged on the ventral side (peritoneal cavity) to observe fluorescence signals for localization within the cervical, axillary, inguinal and popliteal (M, N, O) lymph nodes (LN). Sera were collected from groups of mice on day 7 to determine the rMOMP-specific IgM antibodies using ELISA (P, Q, R). Sera samples were run in triplicates, and experiments were repeated at least three times.

Table 1

Properties of nanoparticles.

Nanoparticles	Zeta-size (nm)	Zeta-potential (mV)	PDI	Encapsulation efficiency	Loading capacity
PLGA-PBS	180.7 ± 2.30	−13.2 ± 0.32	0.135	-	-
PLGA-rMOMP	182.7 ± 3.41	−12.6 ± 0.13	0.109	90%	4.67%